Macromolecular Research (2023) 31:285–297
https://doi.org/10.1007/s13233-023-00137-6

Online ISSN 2092-7673
Print ISSN 1598-5032

ARTICLE

From nano to the macro: tuning hierarchical aggregation of thermoresponsive PEG/PCL-based polyurethanes via molar mass/composition control

Lucas Polo Fonseca[1,2]

Received: 23 September 2022 / Revised: 26 October 2022 / Accepted: 4 November 2022 / Published online: 9 March 2023

Abstract

Amphiphilic hyperbranched polyurethanes (HPUs) based on PEG and PCL are promising for several biomedical applications. However, the lack of control over the molar mass and composition hinders a deep understanding of the aqueous self-assembly of HPUs. In this paper, the control over the HPU molar mass and composition was provided by dynamic urea bond-mediated polymerization (DUBMP), enabling a careful evaluation of their aqueous self-assembly by ^{1}H NMR, DLS, and Cryo-TEM. HPUs containing a single PCL block per chain self-assemble into nanoaggregates ($R_h \approx 10$ nm) in water up to its cloud-point temperature (T_{cp}) of 34 °C. On the other hand, HPUs with more than one PCL block per chain self-assemble into nanoaggregates and their clusters below T_{cp}. In this case, the solution behavior can be tuned by the HPU molar mass. Increasing $\overline{M_w}$ from 4 to 19 kDa, HPUs of similar composition can form colloidally stable cluster suspensions ($\overline{M_w}$ = 4 kDa) and phase separate into a denser liquid aggregate–cluster phase ($\overline{M_w}$ = 7 kDa) or into a highly viscous aggregate-network phase ($\overline{M_w}$ = 19 kDa). This type of control over the hierarchical aggregation of HPUs was reported for the first time and is interesting for biomedical applications.

Graphical abstract

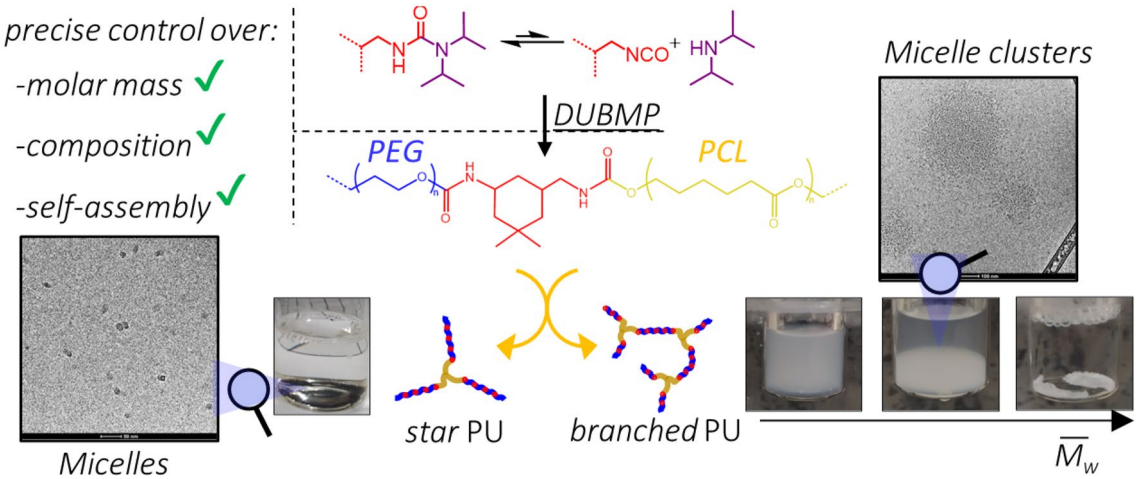

The control of amphiphilic branched PU molar mass and architechture via isocyanate reversible deactivation provided the control over its aqueous phase behavior, tuning it from micelles to micelle-networks

Keywords Polyurethane · Block copolymer · DUBMP · Self-assembly · Amphiphilic · Responsive

✉ Lucas Polo Fonseca
lucas.polodafonseca@ehu.eus

Extended author information available on the last page of the article

1 Introduction

Copolymers based on poly(ethylene glycol) (PEG) and polycaprolactone (PCL) are considered highly promising for several biomedical applications [1, 2]. While PEG confers hydrophilicity, anti-fouling capacity, and hemo-/cyto-compatibility [2–10], the amphiphilic character achieved by its copolymerization with PCL can result in biodegradable materials that can self-assemble in water [1, 4, 8, 11]. Furthermore, both PEG and PCL are FDA-approved polymers for biomedical applications and are produced on a large scale in several countries [1]. However, the synthetic routes that produce PEG/PCL copolymers with a precise architecture and molar mass are complex and usually require toxic solvents, catalysts, inert conditions, and/or several steps, hindering the industrial large-scale production and application of such materials [4, 12–17].

Alternatively, branched polyurethanes (PUs) based on PEG and PCL can be produced by dynamic urea bond-mediated polymerization (DUBMP), which is a one-pot, solvent-, and metal-free synthetic approach [18–20]. DUBMP also improves the control over the PU molar mass and reduces the molar mass dispersity (Đ) values, $Đ \leq 1.8$ for branched PUs and $Đ \leq 1.5$ for linear PUs [18–20]. Telechelic PUs, with both chain-ends of hindered-urea groups, and its PEG-based alternate block copolymers were also produced by DUBMP [19]. Analogous to typical PEG/PCL block copolymers, PEG/PCL-based PUs are also biocompatible and biodegradable [4, 10, 18, 21–25], can be used for the production of hydrogels [4, 18, 21, 23], and also can self-assemble into nano-structures when mixed with water [4, 18, 21, 23]. Besides, PUs based on a vast range of precursors combined with PCL are widely studied materials for biomedical applications, taking advantage of the low toxicity of its bio-degradation products, tunable hydrolysis rates, and mechanical properties [26–29].

Overall, the self-assembly of amphiphilic polyurethanes is described using the amphiphilic block-copolymer self-assembly theory with considerable success [30–32]. Nevertheless, the influence of the isocyanate segments, molar mass, and architecture on the aqueous self-assembly of PEG/PCL-based branched polyurethanes is still poorly understood [4, 10, 22–24]. Despite the considerable amount of studies on the subject of PEG/PCL-based PUs, the majority of them focus on other important properties such as cytotoxicity [1, 4, 24], gelation [4, 18, 21, 23, 25, 33], and so on. Among these, branched PUs are particularly interesting owing to their capacity to form physically crosslinked networks driven by both self-assembly and/or macroscopic phase separation [4, 18, 23]. The presence of hydrophilic and hydrophobic segments distributed along a branched network facilitates the interconnection between hydrophobic or dehydrated domains and, thus, the formation of physical networks [4, 18, 23].

In general, amphiphilic block, or segmented, copolymers that contain more than one hydrophobic segment covalently connected with hydrophilic segments tend to form micellar clusters in aqueous solutions depending on the copolymer concentration [34–37]. This happens due to the presence of different hydrophobic segments from the same macromolecule at different micelle cores, promoting micelle interconnection and leading to clusterization [34–37]. Although this behavior is well understood for amphiphilic multi-block copolymers, to the best of our knowledge, it has not yet been described for amphiphilic multi-block polyurethanes. The lack of control over the structure and molar mass of amphiphilic multi-block PUs can complicate these studies, as it increases the complexity of the PU self-assembly. Herein, DUBMP is a promising tool for overcoming these synthetic challenges [18–21].

Another major challenge when it comes to biomaterials is to achieve hierarchically constructs, such as the ones found in natural tissues, by viable non-toxic synthetic approaches [38–41]. In this paper, we report on the use of tuning the hyperbranched polyurethane (HPU) molar mass and composition via DUBMP to control the self-assembly of such polymers and their hierarchical self-assembly behavior. This control was able to produce stable aggregates, colloidally stable aggregate–clusters, soft viscous aggregate–cluster phases, and highly viscous aggregate networks. The presence of those aggregates and their hydrophobic-effect driven self-assembly were confirmed by combining proton nuclear magnetic resonance (^{1}H NMR), dynamic light scattering (DLS), cryogenic electronic microscopy (Cryo-TEM), and visual assay results of HPU-aqueous solutions below T_{cp}.

2 Experimental section

2.1 Materials

Deuterated chloroform ($CDCl_3$), deuterated water (D_2O), poly(ethylene glycol) (PEG), polycaprolactone-triol (PCL-triol), diisopropylamine (DIPA), and isophorone diisocyanate (IPDI) were purchased from *Sigma-Aldrich*®. Diethyl ether, petroleum ether, and ethanol were purchased from *Synth*®, and tetrahydrofuran HPLC grade was purchased from *Scharlau*®. All reactants were used as received.

2.2 Characterization of the precursors

The absolute number average molar mass ($\overline{M_n}$) of PEG and PCL-triol was determined by the method described by Kricheldorf and Meier-Haack [18, 20, 42]. Briefly, polymer solutions in $CDCl_3$ (5 mg mL^{-1}) were analyzed by ^{1}H

NMR before and after acetylation with trifluoracetic anhydride. The molar mass of the PEG and PCL-triol is shown in Table 1.

2.3 Synthesis and purification procedures

The synthesis of the HPU was described elsewhere [18]. Mixtures of PEG, PCL-triol, DIPA, and IPDI, always with equimolar amounts of DIPA, hydroxyl, and isocyanate groups, and different proportions of PEG and PCL-triol, dependent on the composition, were heated at 100 °C in an SCHOTT® tube under N_2 flow for different times, yielding HPUs of different molar mass. The PEG and PCL-triol content was varied targeting different compositions [18]. The polymers were purified by the dissolution of the reaction medium in ethanol followed by precipitation in a diethyl ether/petroleum ether solution (50% v/v) and drying under vacuum.

The synthesis of the linear PU based on PEG and IPDI via DUBMP was described elsewhere [20]. Briefly, a mixture of PEG and IPDI, with equimolar amounts of hydroxyl and isocyanate groups, was mixed simultaneously at 25 °C with DIPA at different $n_{DIPA}/n_{\text{-NCO}} = 1$ molar ratio. The reaction mixture was then heated to 100 °C in an SCHOTT tube under N_2 flow for 4 h.

2.4 Characterization

The ^{1}H NMR spectra of the HPU in $CDCl_3$ were obtained using a Bruker Avance III HD 250 MHz spectrometer. Solutions of around 5 mg of polymer in 600 µL of $CDCl_3$ were used. The spectrometer was operated with the following acquisition parameters: temperature of 25 °C, pulse width of 11.7 T, pulse delay of 1 s, acquisition time of 3.3 s, and 16 scans with an FID resolution of 0.3 Hz. The ^{1}H NMR analyses of a 0.3 wt% HPU solution in D_2O were performed at 5, 12, and 25 °C on a Bruker Avance II 400 MHz spectrometer using the following acquisition parameters: pulse width of 11.7 T, pulse delay of 1 s, acquisition time of 2 s, and 16 scans with an FID resolution of 0.3 Hz.

Size exclusion chromatography (SEC) analysis was performed in tetrahydrofuran (THF) using a Viscotek GPCmaxVE 2001 chromatograph equipped with a Viscotek VE 3580 RI detector, three Shodex KF-806 M columns, and one Viscotek TGuard 10×4.6 mm guard column and operating at 40 °C. Samples were prepared at 5 mg mL^{-1} of polymer in anhydrous THF and analyzed at a flow rate of 1.0 mL min^{-1}. The number average molar mass ($\overline{M_n}$), mass average molar mass ($\overline{M_w}$), and molar mass dispersity (Đ) were determined using a calibration curve of polystyrene standards purchased from Viscotek with molar masses from 1050 to 3,800,000 Da.

Dynamic light scattering (DLS) experiments were performed on a Zetasizer Nano: Malvern 3600 equipment using a He–Ne laser (632.8 nm) light source and a detector angle of 173°. Silica gel was included in the closed sample compartment for 30 min before the analysis (25 °C) and during the whole experiment to avoid water condensation on the surface of the cuvette when working at temperatures lower than 25 °C. DLS raw data were treated by the constrained regularization method for inverting data (CONTIN) using the *Zetasizer*® software, which provides the number-, volume-, and scattering intensity-based hydrodynamic radius (R_h) distributions.

To address the phase behavior of the HPU-aqueous solutions at 2 wt%, a visual assay was performed. HPU-aqueous solutions were prepared by direct dissolution of the dry polymers in water at 5 °C and kept isothermally at 5 °C for 96 h. After that, the tube inversion test was performed. Samples were then heated to 25 and 37 °C sequentially and then cooled down again to 5 °C followed by vortex stirring. Photos of the samples were taken for all the steps of the assay, which was carried out entirely on a Julabo F12 thermostatic bath for temperature control.

Table 1 Mass (f_x) and molar (x_x) fraction determined by ^{1}H NMR, number of PCL-triol (n_{PCL}) blocks per chain, and the number of PEG blocks per each PCL block (n_{PEG}/n_{PCL}) per chain, both estimated by ^{1}H NMR, $\overline{M_n}$, $\overline{M_w}$, and Đ determined by GPC, and T_{cp} determined by DLS

Code	f_{PEG}/x_{PEG} (wt%/mol%)	f_{PCL}/x_{PCL}	f_{IPDI}/x_{IPDI}	f_{PCL}/f_{PEG}	n_{PCL}	n_{PEG}/n_{PCL}	$\overline{M_n}$	$\overline{M_w}$ (kDa)	Đ	T_{cp}[b] (°C)
PEG	–	–	–		–	–	0.584[a]	1	1.1	–
PCL-triol	–	–	–		–	–	1.238[a]	1.6	1.6	–
HPU_15_6k	61/44	10/3	29/53	0.16	1	15	4.3	6.0	1.39	34[c]
HPU_25_4k	62/47	13/4	25/49	0.21	1 and 2	6	2.3	4.2	1.8	21
HPU_25_7k	57/44	19/7	24/50	0.33	2	6	4.4	7.4	1.7	17
HPU_25_19kk	50/34	16/5	34/61	0.32	4	7	8.3	19.1	2.3	10

[a]Determined by ^{1}H NMR

[b]Determined for 0.0125 wt% aqueous solutions [18]

[c]Determined for 0.3 wt% aqueous solution

Samples for Cryo-TEM analyses were prepared by direct dissolution in deionized water at 5 °C. The HPU solutions at a 3 mg mL^{-1} concentration were deposited onto a Lacey Carbon 300 mesh copper grid (Ted Pella Inc.) in a controlled environment vitrification system (Vitrobot Mark IV, Thermo Fisher Scientific formerly FEI) at 5 °C and 100% humidity. The samples were quickly plunged into a reservoir of liquid ethane at −165 °C. The vitrified samples were then stored in liquid nitrogen until they were transferred to a cryogenic sample holder (Gatan 626) and examined with a JEOL JEM-1400 TEM (120 kV) at about −174 °C. The phase contrast was enhanced by under-focusing. The images were recorded on a Gatan multiscan CCD and processed with Digital Micrograph.

3 Results and discussion

Dynamic urea bond-mediated polymerization (DUBMP) was used to produce HPUs of different compositions based on low molar mass PEG ($\overline{M_n}$ = 584 Da), PCL-triol ($\overline{M_n}$ = 1238 Da), and IPDI. Results showed improved control over the HPU molar mass and Đ relative to conventional synthetic approaches such as polyaddition in solution [18]. The HPUs were amorphous with a single T_g around −37 °C and thermoresponsive, undergoing an LCST-type macroscopic phase separation in an aqueous solution upon heating above the solution cloud-point temperature (T_{cp}). This process led to the formation of a physically crosslinked hydrogel for the HPUs of higher molar mass ($\overline{M_w}$ = 49 kDa) and hydrophobic (PCL) content [18]. The increase in molar mass or the PCL mass fraction decreases the T_{cp}, and the globules formed upon heating above T_{cp} are colloidally stable at 0.0125 wt% [18]. Besides, some evidence suggests that the amphiphilic HPUs based on PEG and PCL self-assemble below their T_{cp} [18, 21]. The attenuation of PCL signals in the ^{1}H NMR of an analogous HPU functionalized with anthracene [21] and the abundance of particles with a hydrodynamic diameter (D_h) of 16 nm, as verified by DLS, suggest that hydrophobic-effect driven self-assembly is occurring [18, 21].

However, no HPU containing a single block of PCL-triol was produced. Besides, despite evidence of HPU self-assembly into stable nano-structures ($R_h \approx 8$ nm) at temperatures lower than the T_{cp}, this behavior was solely investigated by DLS over a short period and for semi-dilute (0.0125 wt%) aqueous solutions [18]. In this paper, a comprehensive study of HPU-aqueous self-assembly in higher concentrations (0.3–2 wt%) and the effect of composition, and molar mass on such a behavior is presented. To do so, an HPU containing a single PCL-triol block per chain (HPU_15_6k) was produced by DUBMP as described in the experimental section. The compositions of all HPUs used in this study determined by ^{1}H NMR, as well as their molar mass determined by gel permeation chromatography (GPC) and the average number of PCL-triol and PEG blocks per chain estimated by ^{1}H NMR and GPC, are presented in Table 1.

The molar mass distribution curve obtained by GPC and the ^{1}H NMR spectra of the HPU_15_6k, as well as the equations used for the HPU mass and molar fractions and estimative of the number of PEG and PCL-triol blocks per chain, are presented in Section I—Structural characterization of the Supporting Information. The GPC curves, $\overline{M_n}$, $\overline{M_w}$,Đ, ^{1}H NMR spectra, and mass and molar fractions of the HPU_25 series were previously reported [18], as well as the DLS data used to determine the T_{cp} of solutions of 0.0125 wt% [18]. DLS data used to determine the T_{cp} of 0.3 wt% HPU_15_6K aqueous solutions are presented in Figure S3—Supporting Information (Section II—Aqueous phase behavior).

Below the T_{cp}, nano-structures of R_h around 8 nm were observed by DLS for aqueous solutions at 0.125 mg mL^{-1} of all the HPUs containing more than one PCL-triol block per chain, as previously reported [18]. The HPU-aqueous solutions at 0.3 wt% were analyzed by DLS at 5 °C (below T_{cp}) at different times after preparation to address the stability of the mixtures. The R_h distribution curves are presented in Fig. 1a. Immediately after solution preparation (0 h), solely scattering objects of $R_h \approx 8$ nm were observed for the HPU_15_6k, HPU_25_4k, and HPU_25_7K, in agreement with what was reported for the 0.01 wt% solutions of HPU_25 [18]. However, HPU_25_19k presented three peaks at $R_h \approx 20$, 200, and 2000 nm at 0 h. For the HPU_15_6k solution, the peak of $R_h \approx 8$ nm stays nearly unchanged after 260 h.

For the HPU_25_4k and HPU_25_7k, isotherms of 90 h below T_{cp} leads to suppression of the peak at $R_h < 50$ nm and to the appearance of a second peak at larger R_h values (Fig. 1b, c). For HPU_25_19k, the peaks shifted to higher R_h values and the peak centered at $R_h = 20$ nm disappeared as well (Fig. 1d). After 260 h at below T_{cp}, only the 0.3 wt% solutions of HPU_15_6k and of HPU_25_4k, which contains 1 PCL block per chain and a mixture of 1 and 2 PCL blocks per chain, respectively, give suitable results for the DLS analysis (Fig. 1a, b). The quality of the results, as well as the temporal increase in R_h of the aggregates of HPU_25 series is also verified in the correlation functions (Fig. 1).

It is hypothesized that the structures of $4 \leq R_h \leq 10$ nm observed by DLS for the HPU at 0 h after preparation are related to micelles with a PCL-core and a shell composed of the PEG-IPDI polyurethane segments. The same hypothesis was raised in our previous studies [18, 21]. However, at low concentrations (≤0.025 wt%), isotherms below T_{cp} do not show change on the DLS R_h distribution curves of the HPU-aqueous solutions [18, 21]. Therefore, the temporal evolution to larger R_h peaks in the DLS results of the HPU_25 series (Fig. 1b–d) suggests the formation of micelle clusters, a self-assembly event highly dependent on the copolymer

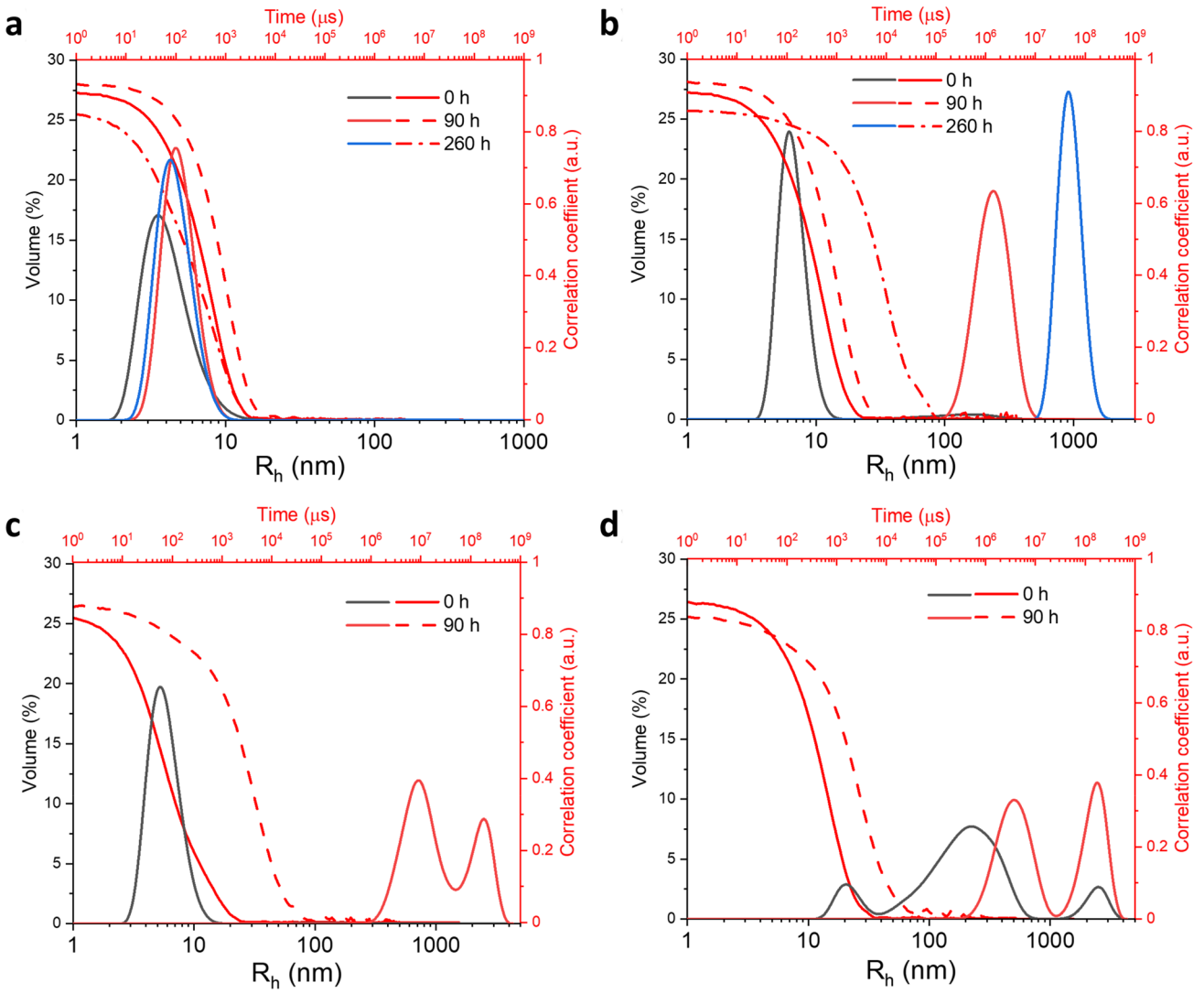

Fig. 1 Volume-based R_h distributions obtained by DLS of **a** HPU_15_6k, **b** HPU_25_4k, **c** HPU_25_7k, and **d** HPU_25_19k aqueous solutions at 5 °C immediately after preparation (0 h) and kept isothermally at 5 °C for different times

concentration [34, 35]. The formation of micelle clusters is related to the presence of multiple hydrophobic blocks per chain, which leads to micelle interconnection due to macromolecules that present hydrophobic segments located at the cores of different micelles [34, 35]. For the HPU_15_6k, aggregate–cluster formation does not occur, and aggregates are thermodynamically stable, probably because this specific composition presents only 1 PCL-triol segment per macromolecule (Table 1), which agrees with micelle formation. The self-assembly for HPU-aqueous solutions below their T_{cp} is schematized in Fig. 2.

Micelle-clusters can interconnect until the formation of micelle networks, which can reach larger sizes (> 5 μm) and, thus, cannot be precisely analyzed by DLS [34, 35]. This happens with the 0.3 wt% aqueous solutions at 5 °C of HPU_25_7k and HPU_25_19k that could not be analyzed by DLS 260 h after their preparation due to the presence of large micro-aggregates ($R_h > 5$ μm). A similar aggregate–cluster formation derived from multiple hydrophobic blocks per copolymer chain was verified for random amphiphilic copolymers of PEG and hydrophobic octadecyl segments [37]. It was found that octadecyl segments can occupy multiple micelle cores, promoting hierarchical micelle aggregation and the formation of micelle clusters [37]. Therefore, the most probable hypothesis is that the nanoaggregates observed by DLS are micelles, with a core composed of PCL-triol blocks, and a shell composed of hydrophilic PEG-IPDI polyurethane segments. A scheme of such hypothesis is presented in Fig. 2. Nevertheless, X-ray scattering experiments need to be conducted to obtain quantitative information regarding aggregate internal structure and the confirmation of micelle (*core–shell*) morphology.

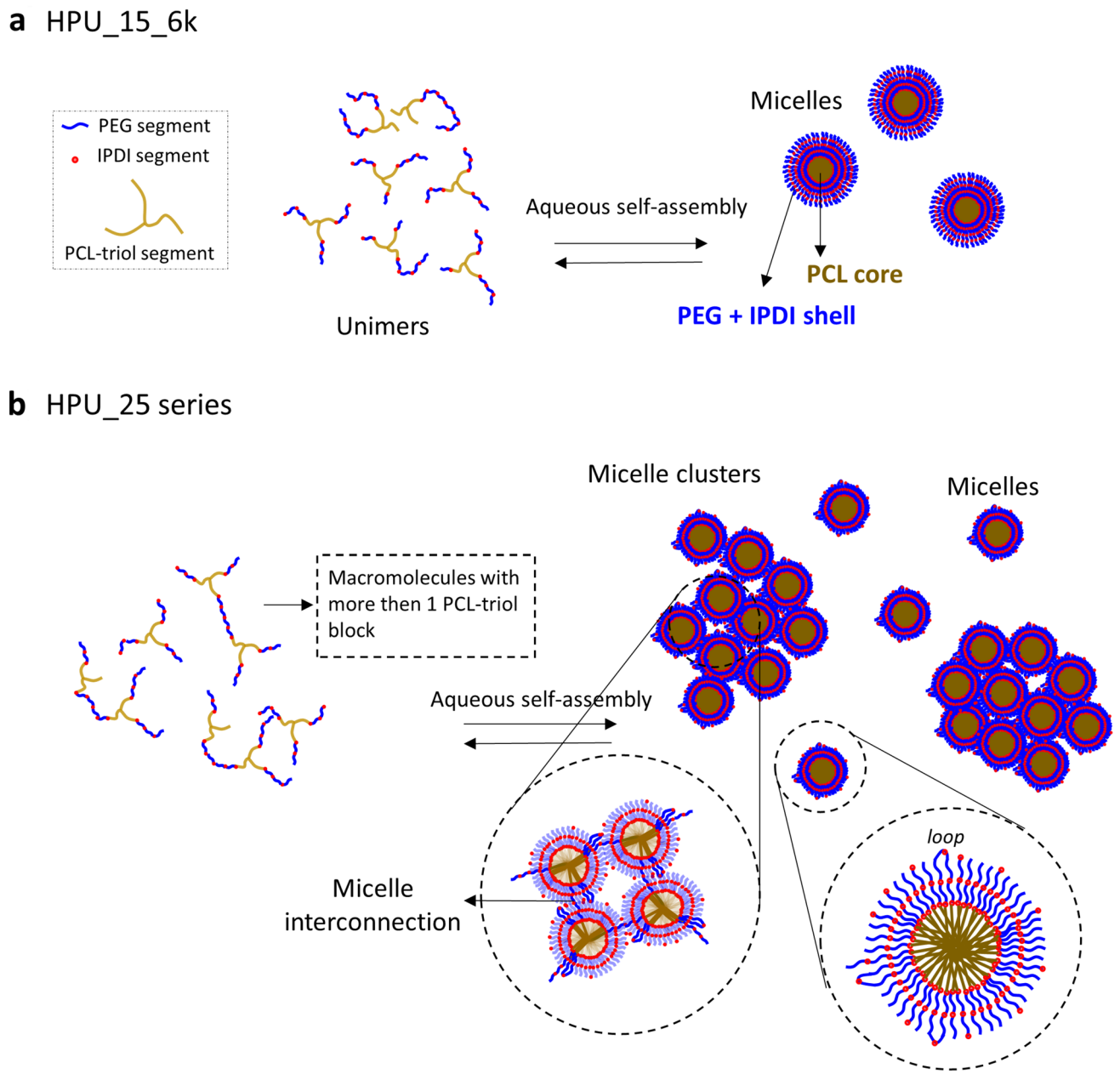

Fig. 2 2D schematic representation of the hypothesis of self-assembly driven micellization of **a** HPU_15_6k, containing only 1 PCL block per chain, and **b** HPU_25 series, containing 2 or more PCL blocks per chain

The stability of the HPU_15_6k aggregate solutions below its T_{cp} and the reversibility of the macroscopic phase separation were also confirmed by comparing different methods of preparation (Figure S3b—Supporting information). Preparing the solution by directly dissolving the dry polymer with cold water (5 °C) or cooling the HPU_15_6k dispersion from temperatures higher than the T_{cp}, to temperatures below T_{cp}, leads to the same DLS result of aggregates with $R_h \approx$ 8 nm (Figure S3b—Supporting information). This agrees with a self-assembly mechanism, and with the hypothesis of micellization [36]. In contrast, the phase behavior of the aqueous solutions of HPU that contains more than 1 PCL block per chain is more complex due to aggregate–cluster formation.

A visual assay of the phase behavior evolution of HPU-aqueous solutions at 2 wt% was carried out by keeping the solutions below T_{cp} for different times, followed by different conditions (Fig. 3). As HPU_15_6k contains one PCL unit per chain, the aggregate solutions are stable, and a clear solution is observed below T_{cp} (Fig. 3a, I–V), agreeing with the hypothesis of micellization [36]. On the other hand, HPU_25_4k, which contains a mixture of chains containing

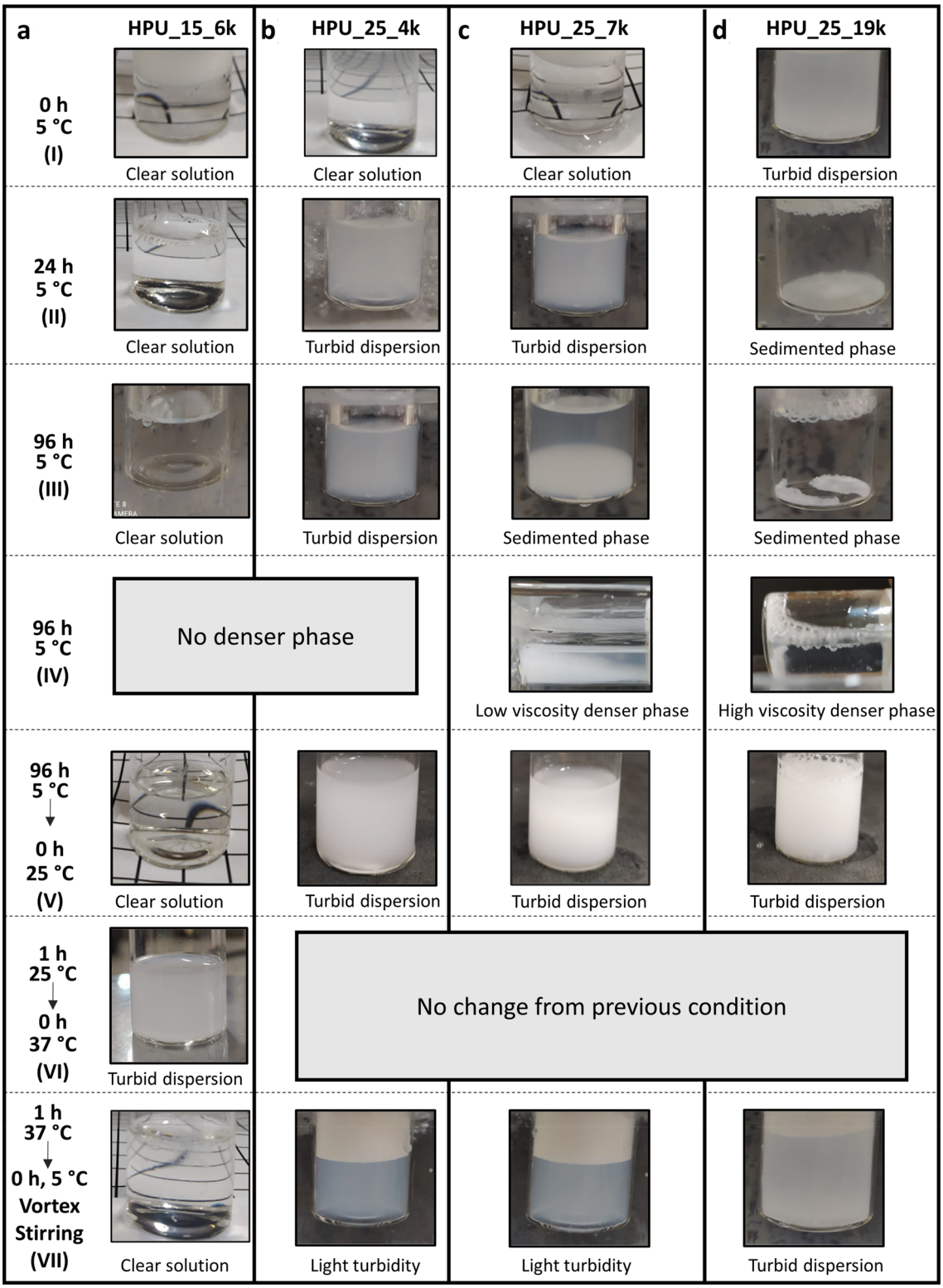

Fig. 3 Photographs of 2 wt% aqueous solutions: **a** HPU_15_6k, **b** HPU_25_4k, **c** HPU_25_7k, and **d** HPU_25_19k, at different conditions applied sequentially from I to VII

1 and 2 PCL blocks per chain, turns from a clear aggregate solution at 0 h after preparation to a turbid aggregate–cluster dispersion at 24 h after preparation (Fig. 3b, I and II). The cluster dispersion of HPU_25_4k is colloidally stable up to 96 h (Fig. 3b, III).

For HPU_25_7k, a cloudy aggregate–cluster dispersion is observed after 24 h (Fig. 3c, II). After 96 h, two phases are observed, one denser opaque phase richer in aggregate–clusters and a slightly turbid phase richer in nanoaggregates (Fig. 3c, III). For the HPU_25_19k, the same event occurs 24 h after preparation (Fig. 3d, II). This result agrees with the hypothesis of clusterization via micelle interconnection. As HPU_25_19k has a higher molar mass and, thus, a higher number of PCL segments per macromolecule compared to HPU_25_7k, micelle interconnections are more abundant leading to larger clusters that rapidly sediment.

Besides, the viscosity of the denser aggregate–cluster phase increases as the molar mass of the HPU_25 series increases, as verified by the tube inversion test (Fig. 3c, d, IV), probably due to the same reason. For instance, in the HPU containing 2 PCL blocks per chain, individual HPU chains can connect at a maximum of two different aggregates. As the number of PCL blocks per chain increases, the HPU individual chains can connect three or more different aggregates. This inevitably leads to a decrease in the mobility of the aggregate–cluster-rich phase, culminating in a highly viscous behavior for the HPU_25_19k (Fig. 3d, IV)

Heating the HPU solutions above T_{cp} leads to turbid dispersions (Fig. 3a–d, V). This result confirms that below T_{cp}, the clear HPU solution phase of the HPU_25_7k and HPU_25_19k aqueous systems (Fig. 3c, d, III) is rich in aggregates. The presence of aggregates and solvated polymer chains in the lower density phase of the HPU_25_7k and HPU_25_19k aqueous systems is mainly a result of the osmotic pressure. Cooling the dispersions below T_{cp} and vortex stirring turn the HPU-aqueous systems to a turbid dispersion state, Fig. 3b–d, VII, except for HPU_15_6k, Fig. 3a, VII, which returns to a clear aggregate solution state even before stirring. Therefore, the aggregate cluster formation is not reversible, the clusters cannot be fully dissociated into aggregates, and clear solutions cannot be obtained again for the HPU_25 series even upon vortex stirring (Fig. 3b–d, VII). This suggests that the clear solution state observed immediately after preparing the solutions from the dry HPU_25_4k and HPU_25_7k is a result of the gradual dissolution of the dry polymer into aggregates/aggregate clusters. Once the polymer concentration becomes high enough, cluster formation takes place irreversibly. Besides, the fully reversible nature of HPU_15_6k LCST macrophase separation agrees with the hypothesis that the nanoaggregates observed below T_{cp} are thermodynamically stable micelles formed upon hydrophobic-effect driven self-assembly [43–45].

To provide additional evidence of HPU aggregation, and insights over its mechanism, ^{1}H NMR measurements were performed for the 0.3 wt% HPU solutions in $CDCl_3$, a good solvent for both PEG and PCL blocks, and on D_2O, a selective solvent for the PEG blocks (Fig. 4). Comparing the spectra for both solvents, Fig. 4, it is clear that there is an attenuation in the PCL and IPDI signals at D_2O for all HPUs. The PCL signal suppression agrees with the hypothesis of hydrophobic-effect-driven micellization [43–45], being a result of the decreased mobility promoted by the highly packed dehydrated PCL chains present in the core of the micelles [43, 46]. However, the IPDI signals were also attenuated, Fig. 4, which is contradictory to the fact that IPDI groups are more abundant in the PEG-IPDI segments located in a hydrated micelle shell at D_2O.

To better understand IPDI signal attenuation, ^{1}H NMR spectra in both D_2O and $CDCl_3$ of a PU containing PEG and IPDI ($\overline{M_w}$ = 11 kDa), synthesized in a previous study [20] and purified by the same procedure as the HPUs, are presented in Fig. 4d. There is no signal attenuation in D_2O for this PU, confirming that both PEG and IPDI are both hydrated. Therefore, IPDI signal attenuation in the HPU ^{1}H NMR spectra in D_2O is a consequence of the hydrophobic-effect-driven self-assembly, led by PCL-triol entropically favored dehydration. Being so, the attenuation of the IPDI signals in the HPU ^{1}H NMR spectra in D_2O is probably related to inter-chain hydrogen bonding present in the shell of the aggregates composed of the hydrated PEG-IPDI polyurethane segments.

Cryo-TEM images of the 0.3 wt% aqueous solutions of HPU_15_6k and HPU_25_7k at 5 °C ($T < T_{cp}$) are presented in Fig. 5. Spherical objects with an average radius of 8 nm were observed in the HPU_15_6k aqueous solution at 5 °C, in agreement with the DLS results (Figs. 1, 5a). This confirms the presence of stable spherical aggregates for the HPU_15_6k, which contains one PCL block per chain. On the other hand, Cryo-TEM images of HPU_25_7k aqueous solutions reveal both spherical particles of an average radius of 4 nm, characterized by the 'darker', higher contrast particles, and clusters of such particles with diameters up to hundreds of nanometers (Fig. 5b). Therefore, Cryo-TEM (HPU_25_7k at 0.3 wt%), as well as the observation of a denser phase formation, macroscopic phase separation process ($T > T_{cp}$) (Fig. 3), DLS, and ^{1}H NMR results, confirm the coexistence of aggregates and aggregate–clusters in the aqueous solutions for the HPU_25 series. At the same time, this results supports the hypothesis of micellization and micelle-cluster formation, although to confirm this hypothesis, X-ray diffraction experiments are required, as previously mentioned [44, 45]. The narrowness of the histograms of the aggregate radius, obtained by Cryo-TEM (Fig. 3) from the diameter measurement of over 140 particles, agrees with the DLS results. The smaller radius of the HPU_25_7k micelles

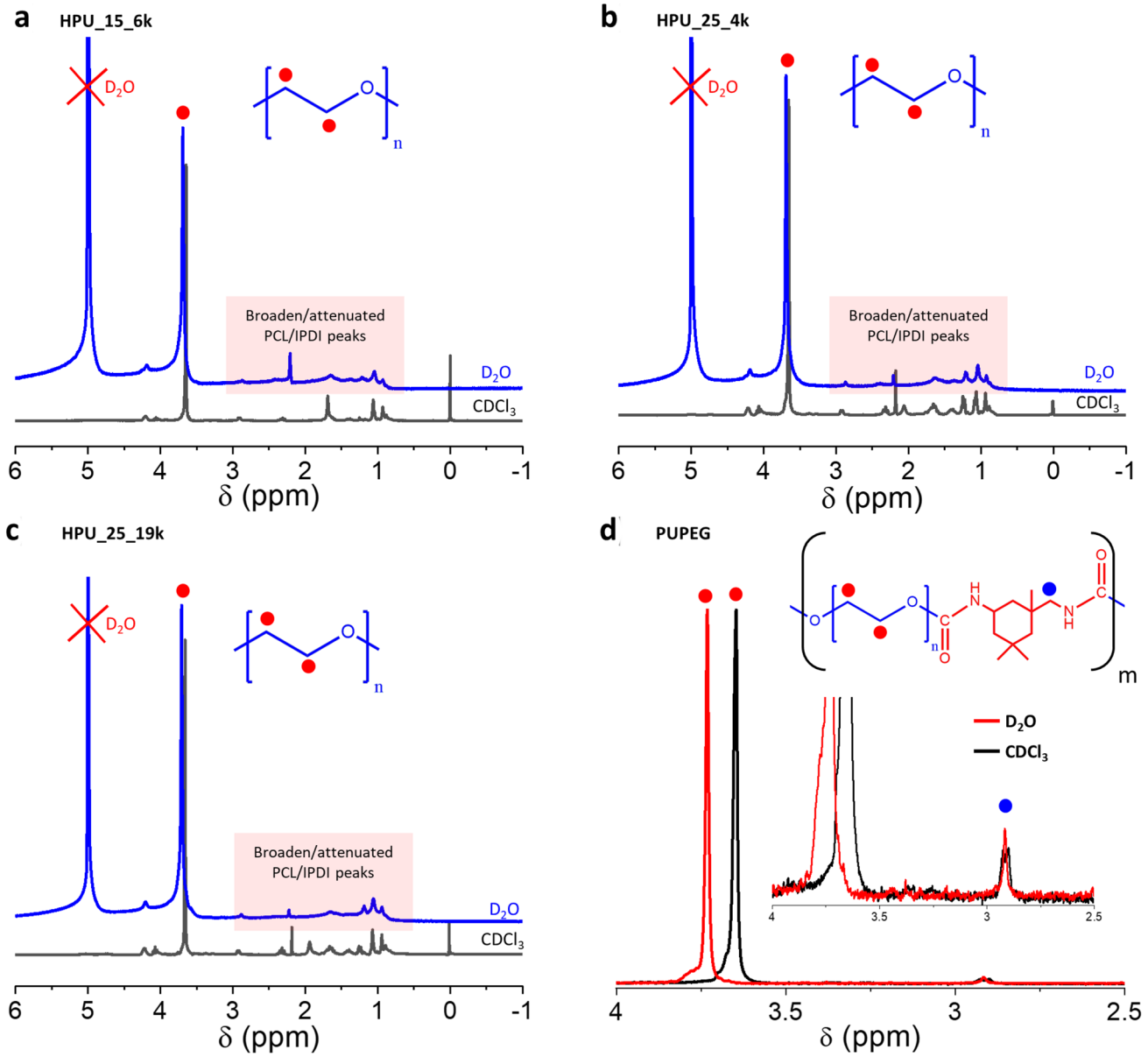

Fig. 4 ^{1}H NMR spectra obtained in $CDCl_3$ and D_2O (5 °C), with intensity normalized by the intensity of the PEG peak (red filled circle), for 0.3 wt% solutions of **a** HPU_15_6k, **b** HPU_25_4k, **c** HPU_25_19k, and **d** PUPEG (colour figure online)

(4 nm), when compared to HPU_15_6k (8 nm), is a result of the higher PCL content of the HPU_25_7k (Table 1). A higher PCL content leads to smaller hydrophilic segments of PEG-IPDI between each PCL-triol segment, comparing both HPU that contains similar $\overline{M}_w$ of 6 and 7 kDa, respectively, for HPU_15_6k and HPU_25_7k. This yields smaller micelle shells for HPU_25_7k and, thus, smaller micelles, considering that the size of the PCL-triol segments is the same on both HPUs. This type of control over hierarchical self-assembly can be useful for biomedical applications, since it allows tunable nano-structures that can favor cell growth, besides potentially allowing for the insertion of localized nanofeatures, such as drugs, cell-signaling agents, and so on, onto the biomaterial [47–49].

4 Conclusion

For the first time, the effect of the composition and molar mass of PEG/PCL-based multi-block branched PU (HPU) in their aqueous self-assembly was investigated thoroughly. While HPUs containing a single block of PCL-triol self-assemble into stable nanoaggregates in aqueous solutions, HPUs containing more than one block of PCL-triol

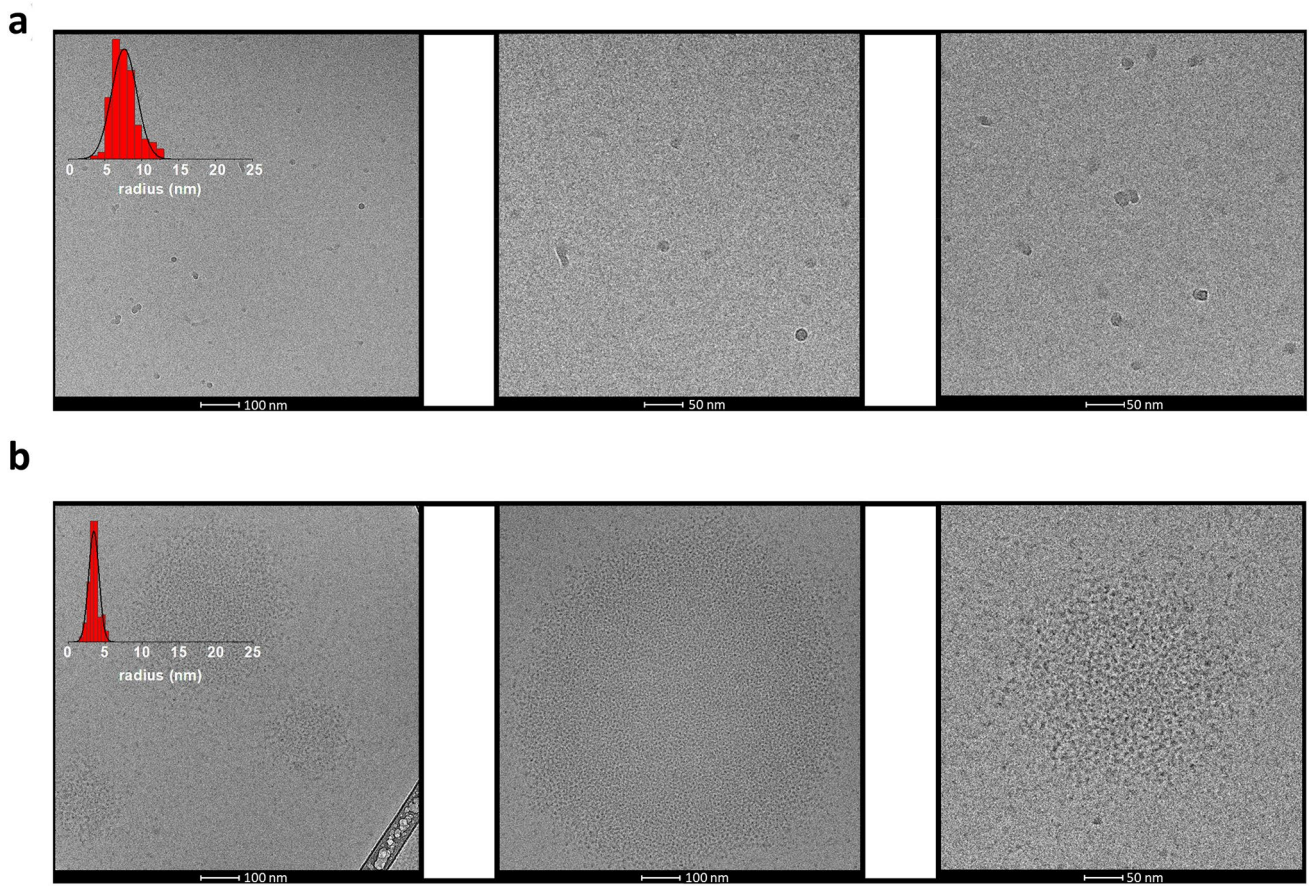

Fig. 5 Cryo-TEM images of 0.3 wt% aqueous solutions of **a** HPU_15_6k and **b** HPU_25_7k at 5 °C

per-chain self-assemble into aggregate–clusters. Both aggregate and aggregate–cluster formation were confirmed by the combination of DLS, ^{1}H NMR, and Cryo-TEM for 0.3 wt% HPU-aqueous solutions, with experiments carried over a time span of 260 h after sample preparation. At a higher concentration (2 wt%), a visual assay showed that aggregate–clusters evolve into a denser aggregate–cluster phase for HPUs containing two or more PCL-triol blocks per chain. Moreover, it was verified that the viscosity of this aggregate–cluster phase is increased by the HPU molar mass and, thus, by the increase in the number of PCL-triol blocks per chain, by favoring the aggregate interconnection. The results agree with the hypothesis of micellization and micelle-cluster formation for the nanoaggregates and aggregate–clusters, respectively, although X-ray scattering experiments need to further be conducted to confirm this hypothesis. Therefore, the PEG/PCL-triol-based branched PU is a promising material for several applications, such as scaffolds, and tissue engineering, especially considering that the hierarchical structure control is a major challenge in such fields. Besides, DUBMP being a solvent/metal-free procedure with improved control over the composition, molar mass, and architecture, relatively to conventional PU synthetic approaches, allows the precise design of HPUs to suit this wide application range.

Supplementary Information The online version contains supplementary material available at https://doi.org/10.1007/s13233-023-00137-6.

Acknowledgements The authors acknowledge FAPESP (Process No. 2015/25406-5) and Coordenação de Aperfeiçoamento de Pessoal de Nível Superior, Brasil (CAPES), Finance Code 001 for the financial support. The authors would like to thank LNNano/CNPEM for the access to the electron microscopy facility and technical support in the execution of the proposal TEM-C2-27165.

Funding Open Access funding provided thanks to the CRUE-CSIC agreement with Springer Nature.

Declarations

Conflict of interest The authors declare that there is no conflict of interest.

References

1. P. Grossen, D. Witzigmann, S. Sieber, J. Huwyler, PEG-PCL-based nanomedicines: a biodegradable drug delivery system and its application. J. Control. Release **260**, 46–60 (2017). https://doi.org/10.1016/j.jconrel.2017.05.028
2. S.A. Senevirathne, K.E. Washington, M.C. Biewer, M.C. Stefan, PEG based anti-cancer drug conjugated prodrug micelles for the delivery of anti-cancer agents. J. Mater. Chem. B **4**(3), 360–370 (2016). https://doi.org/10.1039/c5tb02053k
3. Y. Lu, E. Zhang, J. Yang, Z. Cao, Strategies to improve micelle stability for drug delivery. Nano Res. **11**(10), 4985–4998 (2018)
4. Z. Li, Z. Zhang, K.L. Liu, X. Ni, J. Li, Biodegradable hyperbranched amphiphilic polyurethane multiblock copolymers consisting of poly(propylene glycol), poly(ethylene glycol), and polycaprolactone as in situ thermogels. Biomacromol **13**(12), 3977–3989 (2012). https://doi.org/10.1021/bm3012506
5. G.M.S. Paiva, L.G.T.A. Duarte, M.M. Faleiros, T.D.Z. Atvars, M.I.Z.-E. Felisberti, Isomerization of azobenzene based amphiphilic poly(urethane-urea)s: influence on the dynamic mechanical properties and the effect of the self-assembly in solution on the isomerization kinetics. Eur. Polym. J. **127**, 109583 (2020). https://doi.org/10.1016/j.eurpolymj.2020.109583
6. F. Guo, D. Guo, W. Zhang, Q. Yan, Y. Yang, W. Hong, G. Yang, Preparation of curcumin-loaded PCL-PEG-PCL triblock copolymeric nanoparticles by a microchannel technology. Eur. J. Pharm. Sci. **99**, 328–336 (2017). https://doi.org/10.1016/j.ejps.2017.01.001
7. F. Li, S. Li, A. El Ghzaoui, H. Nouailhas, R. Zhuo, Synthesis and gelation properties of PEG-PLA-PEG triblock copolymers obtained by coupling monohydroxylated PEG-PLA with adipoyl chloride. Langmuir **23**(5), 2778–2783 (2007). https://doi.org/10.1021/la0629025
8. M.S. Sadeghi, M.R. Moghbeli, W.A. Goddard, Self-assembly mechanism of PEG-b-PCL and PEG-b-PBO-b-PCL amphiphilic copolymer micelles in aqueous solution from coarse grain modeling. J. Polym. Sci. **59**(7), 614–626 (2021). https://doi.org/10.1002/pol.20200864
9. J.Z. Wang, M.L. You, Z.Q. Ding, W.B. Ye, A review of emerging bone tissue engineering via PEG conjugated biodegradable amphiphilic copolymers. Mater. Sci. Eng. C **97**, 1021–1035 (2019). https://doi.org/10.1016/j.msec.2019.01.057
10. G. Li, D. Li, Y. Niu, T. He, K.C. Chen, K. Xu, Alternating block polyurethanes based on PCL and PEG as potential nerve regeneration materials. J. Biomed. Mater. Res. Part A **102**(3), 685–697 (2014). https://doi.org/10.1002/jbm.a.34732
11. Y. Yang, C. Hua, C.M. Dong, Synthesis, self-assembly, and in vitro doxorubicin release behavior of dendron-like/linear/dendron-like poly(ε-Caprolactone)-b-poly(ethylene glycol)-b-poly(ε-caprolactone) triblock copolymers. Biomacromol **10**(8), 2310–2318 (2009). https://doi.org/10.1021/bm900497z
12. Z. Luo, L. Jin, L. Xu, Z.L. Zhang, J. Yu, S. Shi, X. Li, H. Chen, Thermosensitive PEG–PCL–PEG (PECE) hydrogel as an *in situ* gelling system for ocular drug delivery of diclofenac sodium. Drug Deliv. **23**(1), 63–68 (2016). https://doi.org/10.3109/10717544.2014.903535
13. S. Peng, H.X. Liu, C.Y. Ko, S.R. Yang, W.L. Hung, I.M. Chu, A hydrolytically-tunable photocrosslinked PLA-PEG-PLA/PCL-PEG-PCL dual-component hydrogel that enhances matrix deposition of encapsulated chondrocytes. J. Tissue Eng. Regen. Med. **11**(3), 669–678 (2017). https://doi.org/10.1002/term.1963
14. H. Wang, D. Tong, L. Wang, L. Chen, N. Yu, Z. Li, A facile strategy for fabricating PCL/PEG block copolymer with excellent enzymatic degradation. Polym. Degrad. Stab. **140**, 64–73 (2017). https://doi.org/10.1016/j.polymdegradstab.2017.04.015
15. C.Y. Gong, S. Shi, P.W. Dong, B. Kan, M.L. Gou, X.H. Wang, X.Y. Li, F. Luo, X. Zhao, Y.Q. Wei, Z.Y. Qian, Synthesis and characterization of PEG-PCL-PEG thermosensitive hydrogel. Int. J. Pharm. **365**(1–2), 89–99 (2009). https://doi.org/10.1016/j.ijpharm.2008.08.027
16. L. Polo Fonseca, R. Bergamo Trinca, M. Isabel Felisberti, Thermo-responsive polyurethane hydrogels based on poly(ethylene glycol) and poly(caprolactone): physico-chemical and mechanical properties. J. Appl. Polym. Sci. **133**(25), 1–10 (2016). https://doi.org/10.1002/app.43573
17. X. Lopez De Pariza, T. Erdmann, P.L. Arrechea, L. Perez, C. Dausse, N.H. Park, J.L. Hedrick, H. Sardon, Synthesis of tailored segmented polyurethanes utilizing continuous-flow reactors and real-time process monitoring. Chem. Mater. **33**(20), 7986–7993 (2021). https://doi.org/10.1021/acs.chemmater.1c01919
18. L. Polo Fonseca, D.D.M.M. Zanata, C. Gauche, M.I. Felisberti, A one-pot, solvent-free, and controlled synthetic route for thermoresponsive hyperbranched polyurethanes. Polym. Chem. **11**(39), 6295–6307 (2020). https://doi.org/10.1039/d0py01026j
19. L. Polo Fonseca, M.I. Felisberti, Dynamic urea bond mediated polymerization as a synthetic route for telechelic low molar mass dispersity polyurethanes and its block copolymers. Eur. Polym. J. **118**, 213–221 (2019). https://doi.org/10.1016/j.eurpolymj.2019.05.052
20. L. Polo Fonseca, Dynamic urea bond-mediated polymerization for solvent-free low-Đ linear polyurethanes of controlled molar mass: hypothesis of diffusion control. Macromol. Chem. Phys. **223**, 2200129 (2022). https://doi.org/10.1002/macp.202200129
21. L. Polo Fonseca, M.I. Felisberti, Thermo- and UV-Responsive amphiphilic nanogels via reversible [4+4] photocycloaddition of PEG/PCL-based polyurethane dispersions. Eur. Polym. J. **160**, 110800 (2021). https://doi.org/10.1016/j.eurpolymj.2021.110800
22. L. Zhou, D. Liang, X. He, J. Li, H. Tan, J. Li, Q. Fu, Q. Gu, The degradation and biocompatibility of PH-sensitive biodegradable polyurethanes for intracellular multifunctional antitumor drug delivery. Biomaterials **33**(9), 2734–2745 (2012). https://doi.org/10.1016/j.biomaterials.2011.11.009
23. Z. Li, J. Li, Control of hyperbranched structure of polycaprolactone / poly (ethylene glycol) polyurethane block copolymers by glycerol and their hydrogels for potential cell delivery. J. Phys. Chem. B **117**, 14763–14774 (2013). https://doi.org/10.1021/jp4094063
24. Y. Yao, D. Xu, C. Liu, Y. Guan, J. Zhang, Y. Su, L. Zhao, F. Meng, J. Luo, Biodegradable PH-sensitive polyurethane micelles with different polyethylene glycol (PEG) locations for anti-cancer drug carrier applications. RSC Adv. **6**(100), 97684–97693 (2016). https://doi.org/10.1039/c6ra20613a
25. M. Boffito, P. Sirianni, A.M. Di Rienzo, V. Chiono, Thermosensitive block copolymer hydrogels based on poly(E-caprolactone) and polyethylene glycol for biomedical applications: state of the art and future perspectives. J. Biomed. Mater. Res. Part A **103**(3), 1276–1290 (2015). https://doi.org/10.1002/jbm.a.35253
26. J. Park, M.J. Lee, G.Y. Ahn, T.H. Yun, I. Choi, E.S. Lee, H. Lee, S.W. Choi, Synthesis and characterizations of biodegradable

polyurethane microspheres with dexamethasone for drug delivery. Macromol. Res. **27**(9), 839–842 (2019). https://doi.org/10.1007/s13233-019-7171-8
27. D. Filip, D. Macocinschi, C.G. Tuchilus, M.F. Zaltariov, C.D. Varganici, Synthesis, characterization of erythromycin propionate core-based star poly(ether urethane)s and their antibacterial properties. Macromol. Res. **29**(9), 613–624 (2021). https://doi.org/10.1007/s13233-021-9069-5
28. E.E. Lopéz-Martínez, J.A. Claudio-Rizo, M. Caldera-Villalobos, J.J. Becerra-Rodríguez, D.A. Cabrera-Munguía, L.F. Cano-Salazar, R. Betancourt-Galindo, Hydrogels for biomedicine based on semi-interpenetrating polymeric networks of collagen/guar gum: synthesis and physicochemical characterization. Macromol. Res. **30**(6), 375–383 (2022). https://doi.org/10.1007/s13233-022-0047-3
29. G. Oh, J. Rho, D.Y. Lee, M.H. Lee, Y.Z. Kim, Synthesis and characterization of electrospun PU/PCL hybrid scaffolds. Macromol. Res. **26**(1), 48–53 (2018). https://doi.org/10.1007/s13233-018-6005-4
30. E.M. Timmers, P.M. Fransen, J.R. Magana, H.M. Janssen, I.K. Voets, Micellization of sequence-controlled polyurethane ionomers in mixed aqueous solvents. Macromolecules **54**(5), 2376–2382 (2021). https://doi.org/10.1021/acs.macromol.0c02107
31. E.M. Timmers, J.R. Magana, S.M.C. Schoenmakers, P. Michel Fransen, H.M. Janssen, I.K. Voets, Sequence of polyurethane ionomers determinative for core structure of surfactant-copolymer complexes. Int. J. Mol. Sci. **22**(1), 1–13 (2021). https://doi.org/10.3390/ijms22010337
32. E.M. Timmers, P.M. Fransen, Á. González García, S.M.C. Schoenmakers, J.R. Magana, J.W. Peeters, R. Tennebroek, I. van Casteren, R. Tuinier, H.M. Janssen, I.K. Voets, Co-assembly of precision polyurethane ionomers reveals role of and interplay between individual components. Polym. Chem. **12**(19), 2891–2903 (2021). https://doi.org/10.1039/d1py00079a
33. L.B. Bronzeri, C. Gauche, L. Gudimard, E.J. Courtial, C. Marquette, M.I. Felisberti, Amphiphilic and segmented polyurethanes based on poly(ε-caprolactone)diol and poly(2-ethyl-2-oxazoline) diol: synthesis, properties, and a preliminary performance study of the 3D printing. Eur. Polym. J. **151**, 1–10 (2021). https://doi.org/10.1016/j.eurpolymj.2021.110449
34. E.V. Razuvaeva, A.I. Kulebyakina, D.R. Streltsov, A.V. Bakirov, R.A. Kamyshinsky, N.M. Kuznetsov, S.N. Chvalun, E.V. Shtykova, Effect of composition and molecular structure of poly(l-lactic acid)/poly(ethylene oxide) block copolymers on micellar morphology in aqueous solution. Langmuir **34**(50), 15470–15482 (2018). https://doi.org/10.1021/acs.langmuir.8b03379
35. E. Kostyurina, J.U. De Mel, A. Vasilyeva, M. Kruteva, H. Frielinghaus, M. Dulle, L. Barnsley, S. Förster, G.J. Schneider, R. Biehl, J. Allgaier, R. Biehl, J. Allgaier, Controlled LCST behavior and structure formation of alternating amphiphilic copolymers in water. Macromolecules **55**(5), 1552–1565 (2022). https://doi.org/10.1021/acs.macromol.1c02324
36. R. Pires-oliveira, J. Tang, A.M. Percebom, C.L. Petzhold, K.C. Tam, E Ff Ect of molecular architecture and composition on the aggregation pathways of POEGMA random copolymers in water. Langmuir (2020). https://doi.org/10.1021/acs.langmuir.0c02538
37. M. Shibata, T. Terashima, T. Koga, Micellar aggregation and thermogelation of amphiphilic random copolymers in water hierarchically dependent on chain length. Eur. Polym. J. **168**, 111091 (2022). https://doi.org/10.1016/j.eurpolymj.2022.111091
38. K. Ariga, L.K. Shrestha, Supramolecular nanoarchitectonics for functional materials. APL Mater. (2019). https://doi.org/10.1063/1.5134530
39. J.D. Halverson, A.V. Tkachenko, Communication: Programmable self-assembly of thin-shell mesostructures. J. Chem. Phys. (2017). https://doi.org/10.1063/1.4999654
40. K. Ariga, X. Jia, J. Song, J.P. Hill, D.T. Leong, Y. Jia, J. Li, Nanoarchitectonics beyond self-assembly: challenges to create bio-like hierarchic organization. Angew. Chemie - Int. Ed. **59**(36), 15424–15446 (2020). https://doi.org/10.1002/anie.202000802
41. Y.K. Go, C. Leal, Polymer-lipid hybrid materials. Chem. Rev. **121**(22), 13996–14030 (2021). https://doi.org/10.1021/acs.chemrev.1c00755
42. H. Kricheldorf, J. Meier-Haack, Polylactones, 22 ABA triblock copolymers of L-lactide and poly(ethylene glycol). Die Makromol. Chemie **194**(2), 715–725 (1993). https://doi.org/10.1002/macp.1993.021940229
43. M. Vamvakaki, D. Palioura, A. Spyros, S.P. Armes, S.H. Anastasiadis, Dynamic light scattering vs 1H NMR investigation of PH-responsive diblock copolymers in water. Macromolecules **39**(15), 5106–5112 (2006). https://doi.org/10.1021/ma0605595
44. K. Kolouchova, O. Sedlacek, D. Jirak, D. Babuka, J. Blahut, J. Kotek, M. Vit, J. Trousil, R. Konefał, O. Janouskova, B. Podhorska, M. Slouf, M. Hruby, Self-assembled thermoresponsive polymeric nanogels for 19F MR imaging. Biomacromol **19**(8), 3515–3524 (2018). https://doi.org/10.1021/acs.biomac.8b00812
45. C.H. Ko, C. Henschel, G.P. Meledam, M.A. Schroer, P. Müller-Buschbaum, A. Laschewsky, C.M. Papadakis, Self-assembled micelles from thermoresponsive poly(methyl methacrylate)-b-poly(N-isopropylacrylamide) diblock copolymers in aqueous solution. Macromolecules **54**(1), 384–397 (2021). https://doi.org/10.1021/acs.macromol.0c02189
46. F. Nardelli, S. Borsacchi, L. Calucci, E. Carignani, F. Martini, M. Geppi, Anisotropy and NMR spectroscopy. Rend. Lincei Sci. Fis. e Nat. **31**, 999–1010 (2020). https://doi.org/10.1007/s12210-020-00945-3
47. N. Karamat-Ullah, Y. Demidov, M. Schramm, D. Grumme, J. Auer, C. Bohr, B. Brachvogel, H. Maleki, 3D printing of antibacterial, biocompatible, and biomimetic hybrid aerogel-based scaffolds with hierarchical porosities via integrating antibacterial peptide-modified silk fibroin with silica nanostructure. ACS Biomater. Sci. Eng. **7**(9), 4545–4556 (2021). https://doi.org/10.1021/acsbiomaterials.1c00483
48. N.A. Sather, H. Sai, I.R. Sasselli, K. Sato, W. Ji, C.V. Synatschke, R.T. Zambrotta, J.F. Edelbrock, R.R. Kohlmeyer, J.O. Hardin, J.D. Berrigan, M.F. Durstock, P. Mirau, S.I. Stupp, 3D printing of supramolecular polymer hydrogels with hierarchical structure. Small **17**(5), 1–14 (2021). https://doi.org/10.1002/smll.202005743
49. G. Le Fer, R.A. Dilla, Z. Wang, J. King, S.S.C. Chuang, M.L. Becker, Clustering and hierarchical organization of 3D printed poly(propylene fumarate)- block-peg- block-poly(propylene fumarate) ABA triblock copolymer hydrogels. Macromolecules **54**(7), 3458–3468 (2021). https://doi.org/10.1021/acs.macromol.1c00132

Authors and Affiliations

Lucas Polo Fonseca[1,2]

[1] POLYMAT and Department of Polymers and Advanced Materials: Physics, Chemistry, and Technology, Faculty of Chemistry, University of the Basque Country UPV/EHU, Paseo Manuel de Lardizabal 3, 20018 Donostia-San Sebastian, Spain

[2] Institute of Chemistry, University of Campinas (UNICAMP), P.O. Box 6154, Campinas, SP 13.084-971, Brazil